J. Electrochem. Sci. Eng. **12(5)** (2022) 865-876; http://dx.doi.org/10.5599/jese.1320

Open Access : : ISSN 1847-9286
https://pub.iapchem.org/ojs/index.php/JESE

Original scientific paper

Corrosion and wear protection of AISI 4140 carbon steel using a laser-modified high-velocity oxygen fuel thermal sprayed coatings

Shanmugasundaram Sivarajan[1,✉], Adwait Joshi[1], Karthikeyan Palani[2], Raghupathy Padmanabhan[1] and Joseph Stokes[3]

[1]*Vellore Institute of Technology, Vandalur Kelambakkam road, Chennai, Pin 600127, India*
[2]*Saveetha Engineering College, Saveetha nagar, Thandalam, Chennai, Pin 602105, India*
[3]*Dublin City University – Glasnevin Campus Dublin 9 - D09 NA55, Ireland*

Corresponding author: ✉*sivarajan.s@vit.ac.in; Tel.: 919841617961*

Received: March 4, 2022; Accepted: June 1, 2022; Published: July 21, 2022

Abstract

Inconel and micro and nano WC-12Co powders were deposited on AISI 4140 carbon steel by high-velocity oxy fuel (HVOF) coating and followed by laser surface modification. Laser power and scan speed were varied at different levels. Microstructure and microhardness were investigated. Nanocoatings performed better than microcoatings. Nanostructured WC powder coatings exhibited greater hardness compared to microstructured powder coating. When the laser power is increased to 170 W, a small cellular dendrite microstructure through multiphase solidification is formed due to the difference in thermal properties of Inconel 625 and WC particles. Adequate laser power and low scan speed were preferred to produce a high-quality coating. From the electrochemical corrosion test results, it was observed that the corrosion rate of laser-modified HVOF sprayed coating is lower than the carbon steel sample. This shows that the Inconel sprayed by laser-modified HVOF coating enhanced the corrosion resistance of the substrate steel material. The porosity percentage was higher for all the samples when laser scan speed was increased.

Keywords
Inconel-625; tungsten carbide; WC-12Co

Introduction

AISI 4140 carbon steel is extensively used in petrochemical and other industrial applications. However, this steel cannot be used in an aggressive corrosive atmosphere due to its poor corrosion resistance. Many coating techniques like physical vapor deposition (PVD), chemical vapor deposition CVD, thermally sprayed coatings, and laser surface modification can be employed to improve the corrosion resistance of carbon steel. Machine component degradation occurs in petrochemical and related industries due to wear and tribo-corrosion. A material deterioration is troublesome to

production and plant workers and expensive to prevent. Many researchers worldwide have tried to combat material degradation by developing new advanced materials. To minimize material degradation, protective coatings produced by the electrolytic hard chromium process are not recommended due to environmental issues. Moreover, water plays a crucial role in hard chrome plating; today, its depletion limits its use [1]. PVD and CVD coatings are not preferred to combat material degradation due to inferior properties and high application costs [2].

Thermal spraying is an extensively used coating technique to protect materials from wear and corrosive atmosphere [3-14]. However, this process induces changes to the coating powder, resulting in defective coatings. Additionally, the oxide formation during thermal spraying can affect the efficiency of coatings in extreme and aggressive surroundings [15]. The adhesive strength between coating and substrate is also not very good in thermal sprayed coatings. Hence, it is unsuitable for protecting the surface of materials in severe conditions. Laser surface modification can be considered a probable technique to minimize the flaws of the coatings. Laser surface modification via heat treatment offers advantages like accurately controlled dimensions, and least heat-affected zones, producing no thermal effects on the substrate. The laser surface modification can also be employed for parts with complex shapes. Furthermore, automation can be easily achieved in laser processing. Laser processing as a post-treatment process for high-velocity oxy fuel (HVOF) coatings to enhance corrosion resistance has been reported by many researchers [16-23].

Nanostructured materials are of great interest because of their superior properties, which differ from bulk materials. Nanostructured WC-12Co powder is used to enhance for wear resistance of various metallic surfaces. Nevertheless, a spray of nano-sized powder is difficult owing to its low weight. Inconel 625 coatings are widely used to improve the corrosion resistance of steel. Inconel 625 coatings find many applications in petrochemical and power generation industries to protect the equipment operating in severe conditions.

The influence of laser heating on the hardness of WC-CoCr HVOF sprayed coating was examined [24]. The average value of the microhardness of the coating increased after laser heating from 1161.7 Hv to 1579.8 Hv. Furthermore, the microhardness is improved with reduced porosity of the coating. Coatings produced by a laser-assisted spraying process; also called laser hybrid spraying, where thermal spraying and laser melting processes were combined to get denser coatings of different Ni-base materials on low carbon steel substrate were reported [25]. Laser-hybrid Inconel 625 coatings showed poor corrosion behavior due to cracks and high iron dilution from the substrate.

The influence of laser melting on the mechanical properties of Inconel 625 and Inconel 625 with WC as MMC HVOF sprayed on 316L steel substrate was investigated [26]. It was observed that wear resistance increases by increasing the percentage of WC in the coating material. The residual stress profile and room temperature wear behavior of WC-Co coatings deposited by kinetic metallization were characterized [27]. The SEM imaging and etched optical micrographs showed significant plastic deformation and particle penetration at the interface due to the high energy impact of feedstock particles. The wear resistance measured by the pin-on-disk method showed a wear performance comparable to conventionally sprayed WC-Co coatings. The laser cladding technology, a modern joining technique to fulfill the requirements of many industrial applications, is reviewed [28]. The purpose is to facilitate researchers by providing comprehensive knowledge about this technology to encourage them to explore it in future research and innovation efforts. It was reported that shorter spray distance and higher fuel flow increased the particle velocity during HVOF spraying of FeMnCrSi coatings [29]. Higher particle velocity showed higher compressive residual stress. The lower powder

feed rate promoted an increase in compressive residual stress. Cavitation wear resistance is higher for higher compressive residual stress.

The performance of two coating processes to combat the water droplet impingement erosion (WDIE) phenomenon was compared [30]. High-velocity air fuel (HVAF) and high-velocity oxygen fuel (HVOF) processes are used to spray WC-10Co-4Cr powder on Ti-6Al-4V. At 250 m/s and 300 m/s, gradual damage occurs due to accumulated impact and jetting, where HVAF outperformed HVOF coating. HVOF's lower performance is attributable to the formation of an unwanted brittle W2C phase. Suspension-high velocity oxygen fuel spraying (S-HVOF) and suspension plasma spraying (SPS) were applied to produce Al_2O_3 coatings using homemade and commercially available Al_2O_3 water-based liquid feedstocks containing 40 wt.% of sub-micrometer-sized raw powders [31]. The influence of feedstock characteristics and spray process conditions on the mechanical and tribological properties was analyzed. Furthermore, the corrosion behavior of superalloys used in turbines is studied and reviewed [32]. Grey cast iron (CI) substrate was coated with Inconel718-based composite coating with a high-velocity oxy-fuel technique [33]. The coating with 10 wt.% Al_2O_3 content exhibited the maximum corrosion resistance. In thermal power plants, protection of materials surface from degradation is crucial since it leads to plant inefficiency [34]. The role of thermal spray coatings has been investigated to protect different steel grades exposed to such degrading conditions at high temperatures in coal-based power plants. The bimodal composite coatings developed with Inconel and Al_2O_3 protect the underlying substrate due to their hardness and fracture toughness [35]. This paper aims to investigate the viability of laser remelting of the HVOF spraying process to coat nano-sized WC-12 Co mixed with Inconel 625 on steel substrates. In addition, the effect of laser parameters on these coatings will be evaluated by microstructure and microhardness measurements.

Experimental

Coating powders

To protect the AISI carbon steel from corrosion and wear, three different powders were used for deposition using HVOF thermally sprayed coating. The first was Inconel-625 (Diamalloy 1005). The chemical composition of Diamalloy 1005 is 66.5 wt.% Ni, 21.5 wt.% Cr, 8.5.wt.% Mo, 3 wt.% Fe and 0.5.wt.% Co. Tungsten carbide WC-12Co (Diamalloy 2004- Sintered) was also used to improve wear resistance. The chemical compositions for (Diamalloy 2004) are 88 wt.% WC and 12 wt.% Co. A nanostructure superfine WC-12Co Infralloy TM S7412 was used in the composite mixture to compare against conventional coatings. Its chemical composition is as follows: 88 wt.% WC and 12 wt.% Co. The substrate material used is made up of AISI 4140 carbon steel. In each sample, two of the three powders were mixed to various compositions, as shown in Table 1.

The coating powders were deposited on AISI carbon steel using an A1050 DJH automated HVOF gun spray device. Grit blasting was performed on these AISI carbon steel samples with the help of honite powder particles. Moisture was removed from steel samples by heating them to 110 °C. The parameters were selected based on the powder composition to avoid decomposition.

Laser equipment and processing parameters

Laser surface modification was carried out on HVOF sprayed steel samples using a pulsed laser system. The CO_2 Rofin laser has a power rating of 1.5 kW. Compressed argon was provided coaxially as a shielding gas. The PRF (pulse repetition frequency) was kept constant at 400 Hz. The focal point position was kept at –5 mm. In the first set of six experiments, the laser power was varied at six

levels at a constant scan speed of 1000 mm min^{-1}. Laser power levels used were 20, 55, 105,170, 240, and 290 W. In the second set of experiments, the laser scanning speed varied at six levels at a constant laser power of 55 W. Scanning speed levels were 750, 1000, 1250, 1500, and 2000 mm min^{-1}. In addition, the scanning electron micrographs were taken.

Table 1. *Composition of powders in sample*

Sample	Content, wt.%		
	WC-12Co (nano)	WC-12Co (micro)	Inconel 625 (micro)
S1	25	0	75
S2	50	0	50
S3	75	0	25
S4	0	75	25
S5	0	50	50
S6	0	25	75

Mechanical characterization of coatings

The hardness of the coatings was measured by Vickers microhardness testing machine manufactured by SHIMADZU (Model: HMV-G). The resolution was 0.01 µm, and the load used was 100 g. The duration of the load applied was 10 seconds. Indentation was made on different parts of the heat-affected zone and the shape of indentation observed was of the rhombus. The length of both the diagonals was measured and based on that measurement Vickers hardness number was directly calculated and graphs plotted. Three sets of readings were taken to ensure consistency in results.

Electrochemical corrosion tests

The Tafel tests of laser-modified HVOF sprayed sample and carbon steel sample were performed in salt solution at 36.5 °C using a potentiostat (Interface 1010, Gamry Instruments) by exposing 0.375 cm^2 area of the samples. The corrosion cell consists of a saturated calomel electrode (SCE) and a platinum wire as reference and counter electrodes. Tafel plots were created by polarizing the specimen about 0.3 V anodically and cathodically with reference to open circuit potential (OCP) at a scan rate of 0.5 mV s^{-1} after an initial delay of 60 minutes. After the measurements were obtained, the Tafel data were analyzed by curve fitting and equivalent circuit modeling using Gamry Echem Analyst software.

Porosity measurement

Assuming that resolution limits are considered, porosity within a microstructure can be easily detected by image analysis due to the high degree of contrast between the dark pores (voids) and the more highly reflective coating material. In this study, the SEM images were used to check the porosity using ImageJ software. The areas of porosity were selected in the SEM image and the percentage of porosity was analyzed and processed by ImageJ software

Results and discussion

The detailed microstructure analysis of HVOF sprayed WC-12Co-Inconel-625 coatings exhibits spat-like layered morphologies due to the re-solidification of molten and semi-molten powder particles. During HVOF spraying, WC-12Co-Inconel 625 coatings under different powder compositions contain three distinct zones: fully, partially, and unmelted core. The formation of molten, semi-molten and unmelted zones is due to variation in melting temperature of WC-12Co and Inconel particles relative to flame temperature. The formation of three separate zones was confirmed by

previous research work [36]. In addition, defects such as pores, micro defects and cracks are found in most HVOF coatings.

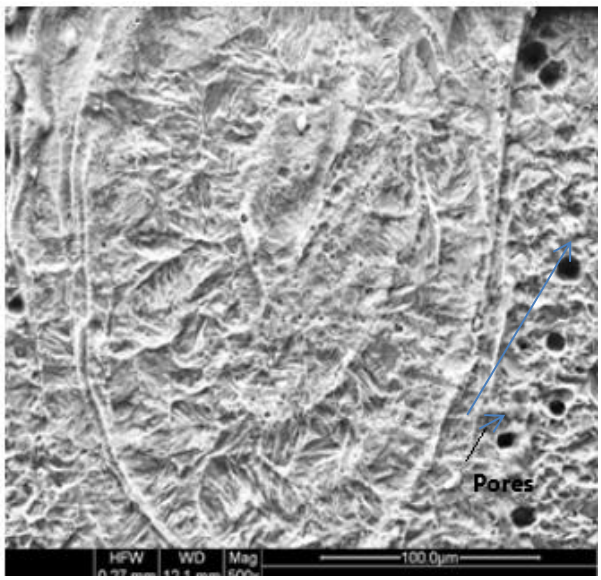

***Figure 1**. SEM image of laser-modified HVOF thermally sprayed Inconel 625 and WC-12Co coatings; laser power = 55 W; laser scan speed = 1000 mm min^{-1} microstructured powder*

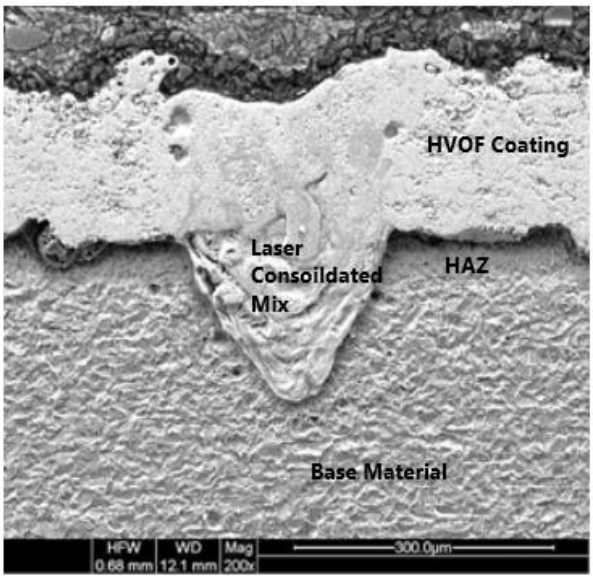

***Figure 2**. SEM Image of laser-modified HVOF thermally sprayed Inconel 625 and WC-12Co coatings; laser power = 55 W; laser scan speed = 1500 mm min^{-1} microstructured powder*

Partially molten and fully molten particles of HVOF coatings were modified by laser with a reduction in cracks and porosity. The minimization of discrete splats and porosity by laser modification will improve the wear resistance. Figure 1 shows the SEM image of laser-modified HVOF coating with laser power of 55 Watts and a scan speed of 1000 mm min^{-1}. It can be seen that the pores present in the HVOF coating are minimized to a larger extent in the laser-modified zone. Also, the pore size is considerably reduced compared to those present elsewhere. The occurrence of porosity is minimal in the laser-treated region compared to other regions, as can be observed in Figure 2. The SEM image (Figure 2) also shows that the diffusion of coating constituents into the substrate is less, which has helped maintain the original properties of coatings. Improved material consolidation is found to be more effective through laser. Figure 3 shows the SEM image of the coatings in which splats, pores, and cracks are visible in the microstructure. This is because the laser power is too low to melt WC and Inconel particles with nanostructured powder. Figure 4 shows an SEM image of coating in which a fine-grained homogenous poly phase microstructure is developed due to low laser scan speed while maintaining low laser power (55 W).

When the laser power is increased to 170 W, a small cellular dendrite microstructure through multiphase solidification is formed due to the difference in thermal properties of Inconel 625 and WC particles, as observed in Figure 5. The surface is made up of coating material and the substrate, leading to a differential cooling rate; hence, the cell size and orientation vary in the coating [37-38]. Figure 6 shows the SEM image in which large pores are seen due to higher scan speed. When the scan speed and power are high, the time of contact is less and there is less time for the gases and bubbles formed during the coating powder reactions to escape, resulting in pores in the coating remelting zone. A dendrite microstructure is observed at higher magnification in the SEM image due to multiphase solidification, as shown in Figure 7.

***Figure 3**. SEM image of laser modified HVOF thermally sprayed Inconel 625 and WC-12Co coatings; laser power 55 W laser scan speed = 1250 mm min^{-1} nanostructured powder*

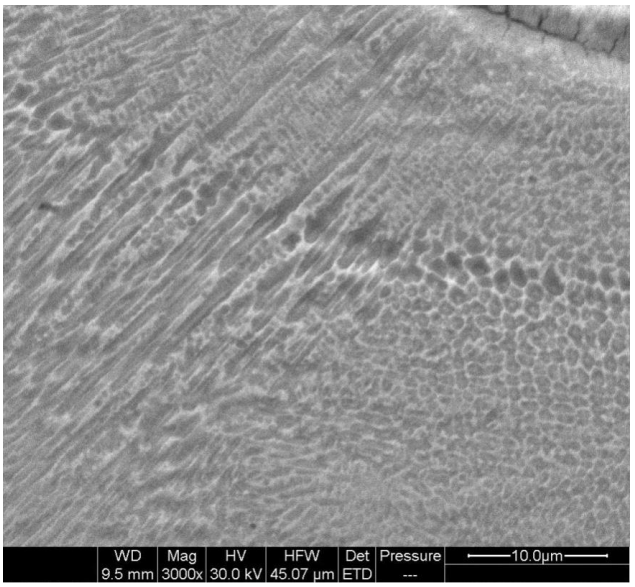

***Figure 4.** SEM image of laser modified HVOF thermally sprayed Inconel 625 and WC-12Co coatings; laser power 55 W laser scan speed = 1000 mm min^{-1} nanostructured powder*

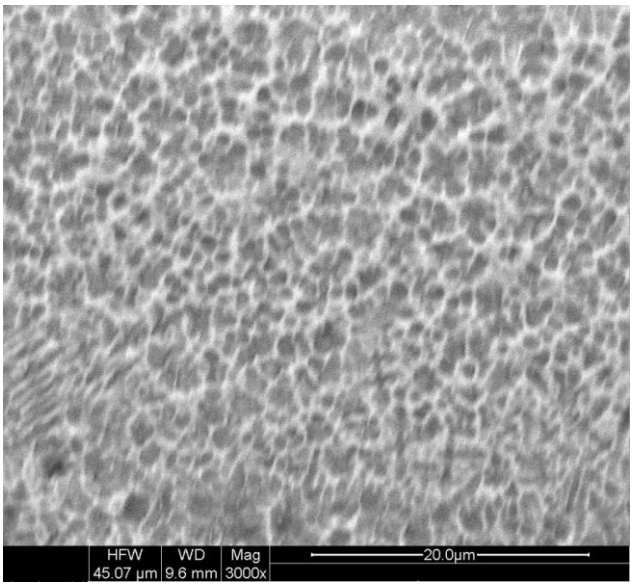

***Figure 5**. SEM image of laser modified HVOF thermally sprayed Inconel 625 and WC-12Co coatings; laser power 170 W. laser scan speed = 1500 mm min^{-1}. nanostructured powder*

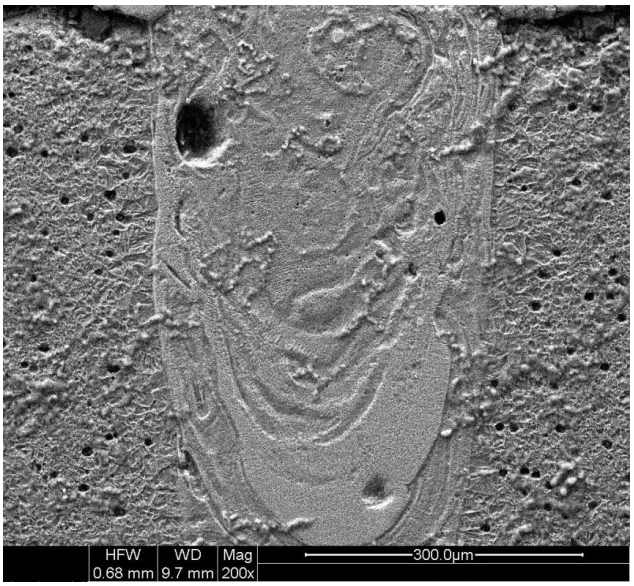

***Figure 6**. SEM image of laser modified HVOF thermally sprayed Inconel 625 and WC-12Co coatings; laser power 170 W. laser scan speed 1750 mm min^{-1}. micro structured powder*

The influence of laser scan speed on the microhardness of laser melted high-velocity oxy fuel coated samples is shown in Figure 8. The first three coated samples (nano-sized powder coatings) showed higher hardness than the remaining three coated samples (micro-sized powder coatings). The maximum hardness with nano powder coatings is Hv1199 and with micro-sized powder coatings, it is Hv775. Nano powder coatings exhibited better melting leading to the dense coating of higher microhardness. When the laser scan speed was between 1250 to 2000 mm min^{-1}, proper powder melting and consolidation took place, resulting in uniform high microhardness in all three cases. The

influence of laser power on the microhardness of laser melted high-velocity oxy fuel coated samples is shown in Figure 9. When laser power is increased, the micro-hardness of coated samples improves. An increase in laser power combined with low scan speed ensures proper melting and less porosity, leading to high hardness. It was observed that coatings produced by spraying nanopowders show higher hardness than coatings produced by micro-sized powders.

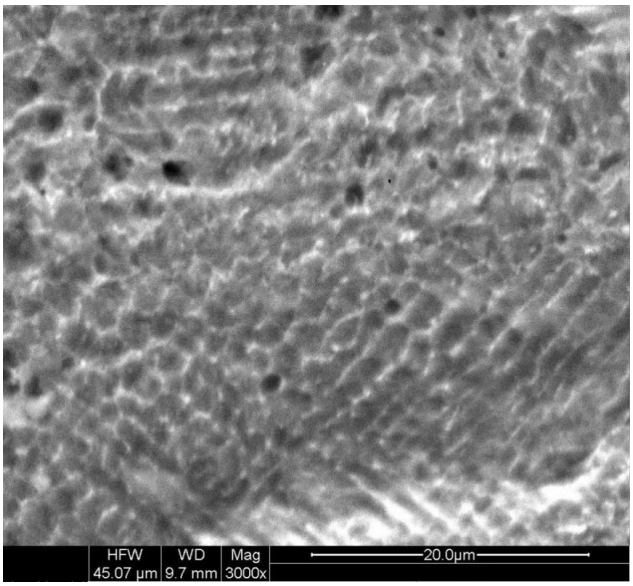

Figure 7. *SEM Image of laser modified HVOF thermally sprayed Inconel 625 and WC-12Co coatings; laser power = 170 W. laser scan speed = 1750 mm min^{-1}. nanostructured powder*

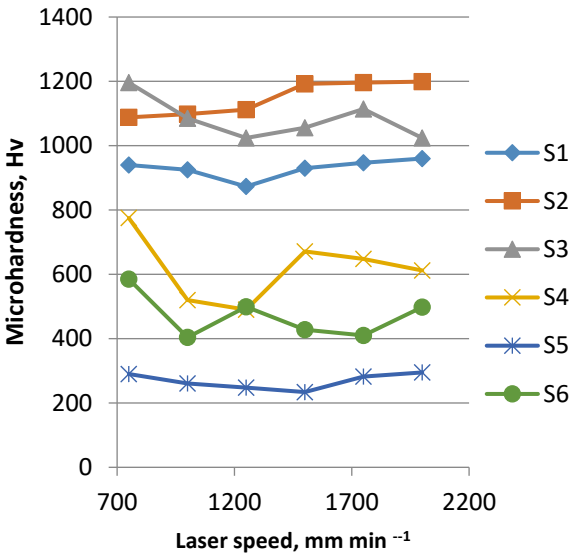

Figure 8. *Variation of microhardness of coatings with laser scan speed; Laser power = 55 W*

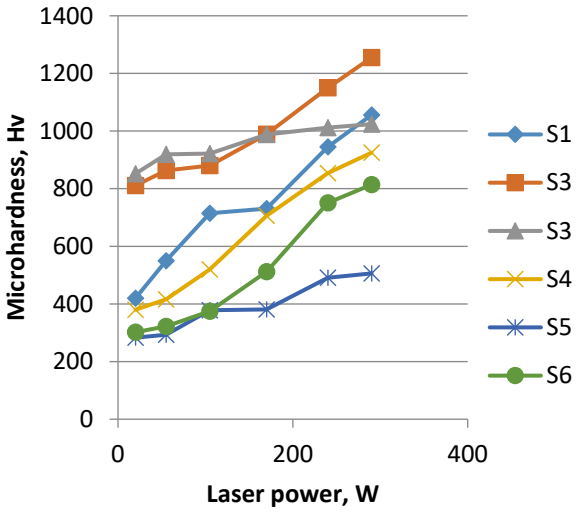

Figure 9. *Variation of microhardness of coating with laser power; laser scan speed = 1000 mm min^{-1}*

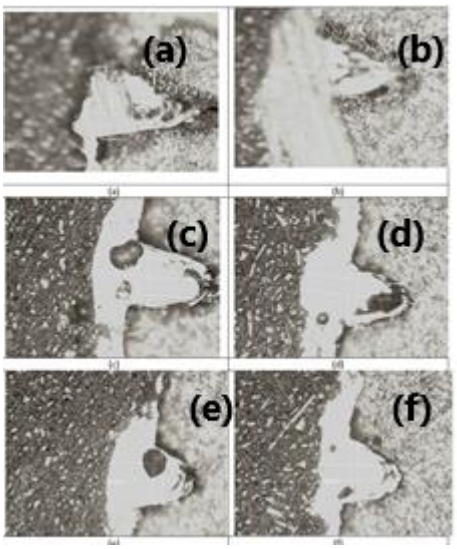

Figure 10*. Microscopic pictures of laser modified HVOF sprayed WC-12CO-Inconel coatings. Sample S1; laser power = 55 W; laser scan speed: (a) 750 (b) 1000 (c) 1250 (d) 1500 (e) 1750 (f) 2000 mm min^{-1}*

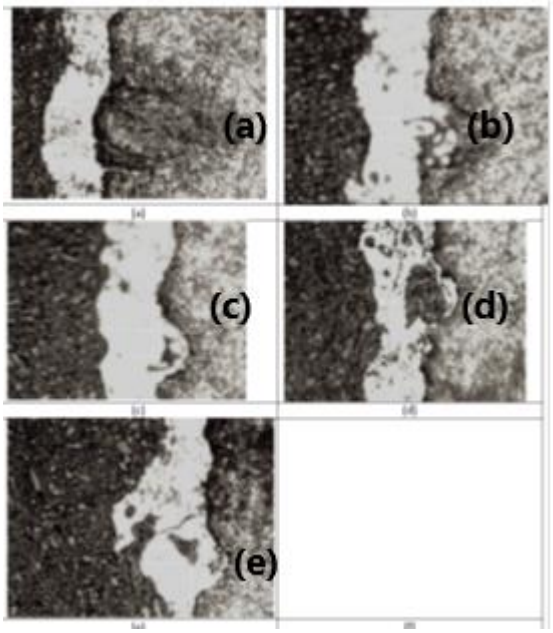

***Figure 11**. Microscopic pictures of laser-modified HVOF sprayed WC-12CO-Inconel coatings; sample S2; laser power = 55 W.; laser scan speed: (a) 750 (b) 1000 (c) 1500 (d) 1750 (e) 2000 mm min^{-1}*

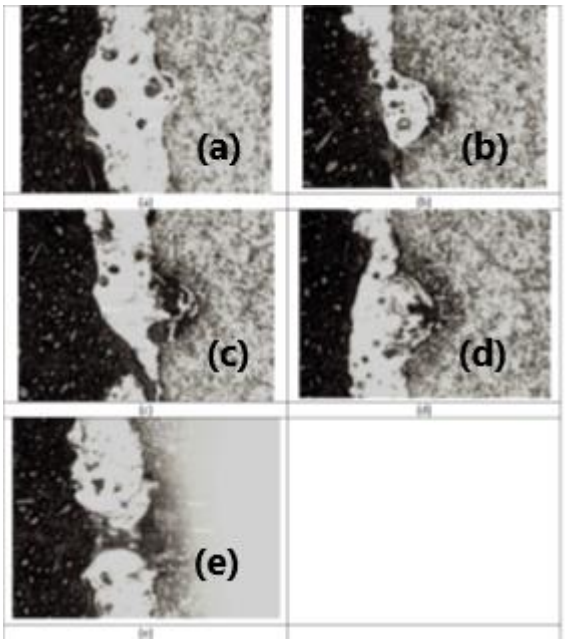

***Figure 12.** Microscopic pictures of laser-modified HVOF sprayed WC-12CO-Inconel coatings; sample S3; laser power = 55 W.; laser scan speed: (a) 750 (b) 1000 (c) 1250 (d) 1500 (e) 1750 mm min^{-1}*

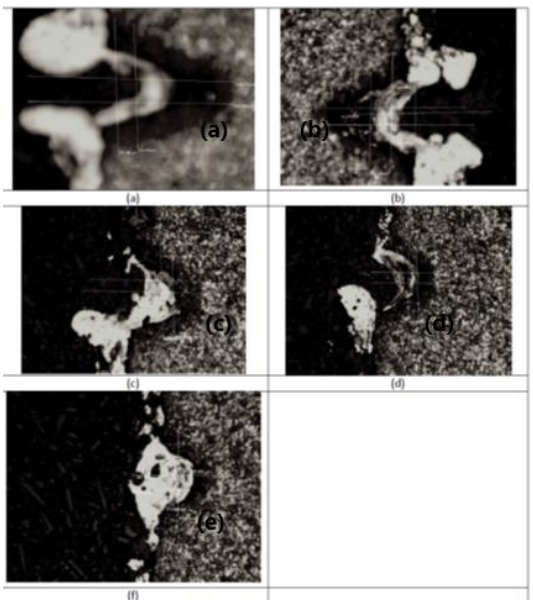

***Figure 13.** Microscopic pictures of laser-modified HVOF sprayed WC-12CO-Inconel coatings; sample S; laser power = 55 W; laser scan speed: a) 750 (b) 1000 (c) 1250 (d) 1500 (f) 2000 mm min^{-1}*

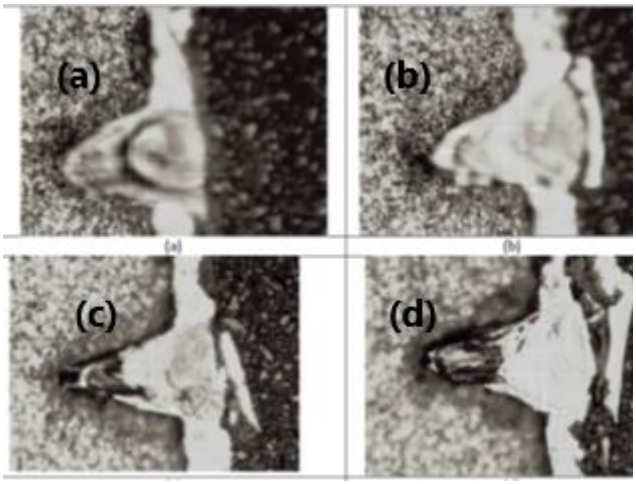

***Figure 14**. Microscopic pictures of laser-modified HVOF sprayed WC-12CO-Inconel coatings, sample S5; laser power = 55 W; laser scan speed: (a) 750 (b) 1000 (c) 1250 (d) 1500 mm min^{-1}*

From the electrochemical corrosion test results (Table 2 and Figure 17), it was observed that the laser-modified HVOF sprayed coating exhibited lower corrosion current density when compared with the plain carbon steel sample. The corrosion rate of laser-modified HVOF sprayed coating is also lower than that of the carbon steel sample. This shows that the Inconel sprayed by laser-modified HVOF coating has enhanced the corrosion resistance of the substrate steel material.

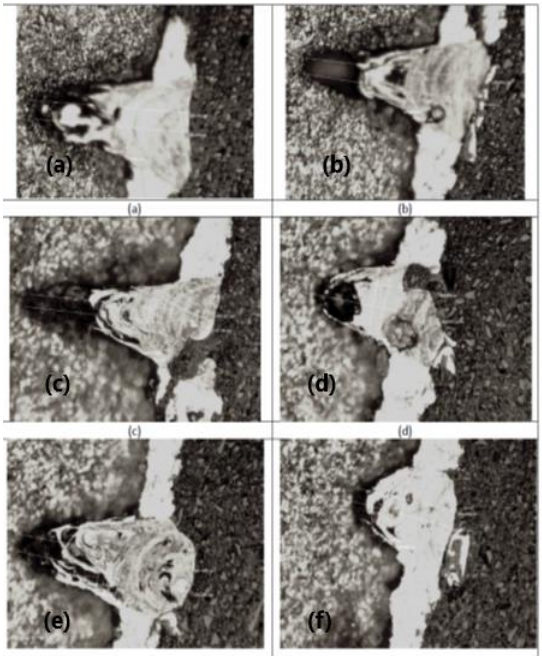

Figure 15. *Microscopic pictures of laser-modified HVOF sprayed WC-12CO-Inconel coatings.; sample S6; laser power 55 W; laser scan speed: (a) 750 (b) 1000 (c) 1250 (d) 1500 (e) 1750 (f) 2000 mm min^{-1}*

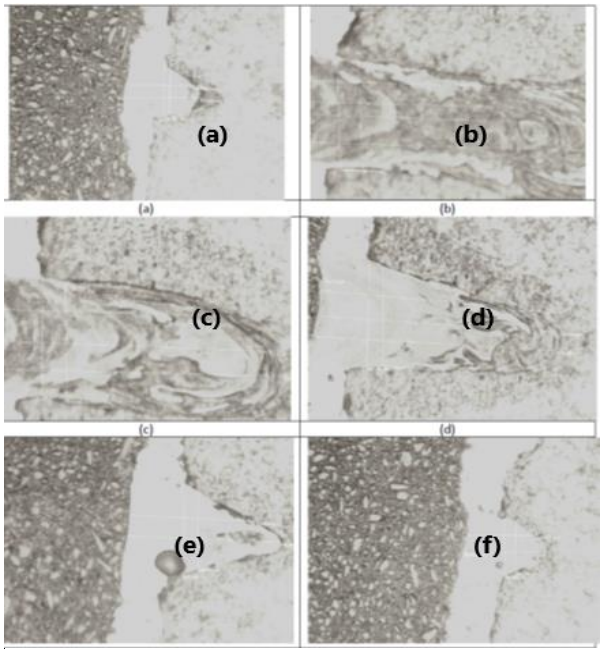

Figure 16*. Microscopic pictures of laser-modified HVOF sprayed WC-12CO-Inconel coatings; sample S1; laser scan speed: 1000 mm min^{-1}; laser power: (a) 20 (b) 55 (c) 105 (d) 170 (e) 240 (f) 290 W*

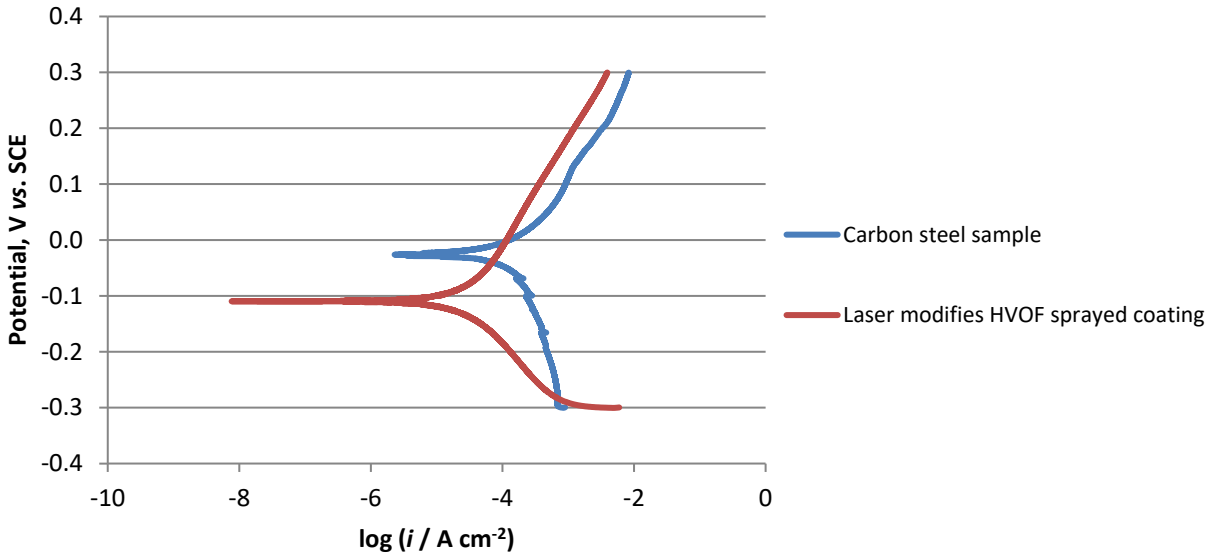

Figure 17. *Tafel curve of laser modified HVOF sprayed coating and carbon steel substrate during the corrosion tests*

Table 2. *Electrochemical corrosion tests results*

	Laser-modified HVOF sprayed sample	Carbon steel sample
i_{corr} / μA cm^{-2}	22.10	808.0
E_{corr} / mV	-110.0	-27.00
Corrosion rate, mm year^{-1}	0.26035	9.53262

Table 3. *Porosity measurement results*

Sample	Laser power, W	Laser scan speed, mm min^{-1}	Porosity, %	Sample	Laser power, W	Laser scan speed, mm min^{-1}	Porosity, %
S1	55	750	1.300	S4	55	750	1.951
S1	55	1000	1.780	S4	55	1000	2.130
S1	55	1250	2.186	S4	55	1250	2.550
S1	55	1500	2.753	S4	55	1500	2.980
S1	55	1750	3.020	S4	55	1750	3.921
S1	55	2000	4.124	S4	55	2000	5.128
S1	20	1000	2.110	S4	20	1000	3.021
S1	55	1000	2.770	S4	55	1000	2.982
S1	105	1000	1.991	S4	105	1000	2.100
S1	170	1000	2.670	S4	170	1000	2.990
S1	240	1000	3.121	S4	240	1000	3.050
S1	290	1000	2.770	S4	290	1000	3.100
S2	55	750	2.100	S5	55	750	2.020
S2	55	1000	2.320	S5	55	1000	2.760
S2	55	1250	2.952	S5	55	1250	3.320
S2	55	1500	2.380	S5	55	1500	3.641
S2	55	1750	3.456	S5	55	1750	4.124
S2	55	2000	3.950	S5	55	2000	4.985
S2	20	1000	2.220	S5	20	1000	2.650
S2	55	1000	2.780	S5	55	1000	2.550
S2	105	1000	2.640	S5	105	1000	2.450
S2	170	1000	2.561	S5	170	1000	3.050
S2	240	1000	1.792	S5	240	1000	2.760
S2	290	1000	2.650	S5	290	1000	3.110
S3	55	750	1.890	S6	55	750	2.123
S3	55	1000	1.720	S6	55	1000	2.520
S3	55	1250	2.456	S6	55	1250	3.820
S3	55	1500	2.670	S6	55	1500	3.621
S3	55	1750	3.222	S6	55	1750	4.980
S3	55	2000	3.992	S6	55	2000	5.320
S3	20	1000	2.051	S6	20	1000	2.990
S3	55	1000	2.221	S6	55	1000	3.290
S3	105	1000	2.781	S6	105	1000	2.870
S3	170	1000	2.450	S6	170	1000	2.560
S3	240	1000	2.680	S6	240	1000	2.740
S3	290	1000	2.730	S6	290	1000	2.690

The porosity measurement is made using ImageJ software [39]. The average porosity of nano samples (S1, S2, S3) is 2.59 % and the average porosity is 3.13 %. In all six samples, the porosity increased with an increase in laser scan speed. When the scan speed and power are high, the time of contact is less and there is less time for the gases and bubbles formed during the coating powder reactions to escape and this has resulted in the occurrence of pores in the coating remelting zone.

Conclusions

In conclusion, WC powder particle size, laser power and laser scan speed were varied, and its effects on the microhardness and microstructure developed in the coating were examined. Micro-Hardness measurements performed on laser-modified HVOF coatings displayed constantly greater values for coatings produced by nanopowder compared to coatings made by micro powder. When the laser power is increased to 170 W, a small cellular dendrite microstructure through multiphase solidification is formed due to the difference in thermal properties of Inconel 625 and WC particles.

Adequate laser power and low scan speed will be preferred to produce a coating with high quality. The electrochemical corrosion test results showed that the corrosion rate of laser-modified HVOF sprayed coating is lower than the carbon steel sample. This shows that the Inconel sprayed by laser-modified HVOF coating has enhanced the corrosion resistance of the substrate steel material. The porosity percentage is higher for all the samples when laser scan speed increases. Therefore, for AISI 4140 carbon steel, to improve the wear and corrosion resistance, laser-modified HVOF nano-sized WC-12Co –Inconel-625 coatings show the promising result.

Acknowledgements: *The authors would like to express their sincere gratitude to Vellore Institute of Technology, Chennai, India and Dublin City University, Ireland for the support given in carrying out this research work. The authors would like to express their sincere gratitude to Dr. R. Radha and Mr. Babu of Materials Engineering Lab of Vellore Institute of Technology, Chennai, India for their support in performing electrochemical corrosion tests.*

References

[1] S. Abdi, S. Lebaili, *Physics Procedia* **2** (2009) 1005-1014. https://doi.org/10.1016/j.phpro.2009.11.056

[2] T. S. Sidhu, S. Prakash, R. D. Agrawal, *Surface and Coatings Technology* **201** (2005) 273-281. https://doi.org/10.1016/j.surfcoat.2005.11.108

[3] D. Chidambaram, C. R. Clayton, M. R.Dorfman, *Surface and Coating Technology* **176(3)** (2004) 307-317. https://doi.org/10.1016/S0257-8972(03)00809-0

[4] E. Chikarakara, S. Aquida, D. Brabazon, S. Naher, S. J. A. Picas,M. Punset , A. Forn, *International Journal of Material Forming* **3** (2010) 801-804. https://doi.org/10.1007/s12289-010-0891-0

[5] T. S. Sidhu, S. Prakash, R. D. Agrawal, *Surface and Coating Technology* **200** (2006) 5542-5549. https://doi.org/10.1016/j.surfcoat.2005.07.101

[6] K. Kanchan Kumari, K. Anand, M. Bellacci, M. Giannozzi, *Wear* **268** (2010) 1309-1319. https://doi.org/10.1016/j.wear.2010.02.001

[7] S. At-Mutairi, M. S. J. Hashmi, B. S. Yilbas, J. Stokes, *Surface and Coating Technology* **264** (2015) 175-186. https://doi.org/10.1016/j.surfcoat.2014.12.050

[8] I. Iordanova, M. Surtchev, K. S. Forcey, *Surface and Coatings Technology* **139** (2001) 118-126. https://doi.org/10.1016/S0257-8972(01)00991-4

[9] H.S.Grewal, H.Singh, Anupam Agrawal, *Surface and Coatings Technology* **216** (2013) 78-92. https://doi.org/10.1016/j.surfcoat.2012.11.029

[10] T. Sahraoui, S. Guessasma, A. Jeridane, M. Hadji, *Materials and Design* **31** (2010) 1431-1437. https://doi.org/10.1016/j.matdes.2009.08.037

[11] M. Ashokkumar, D. Thirumalaikumarasamy, P. Thirumal, R. Barathiraja, *Materials Today Proceedings* **46(17**) (2021) 7581-7587. https://doi.org/10.1016/j.matpr.2021.01.664

[12] A. S. Bolokang, M. Ntsoaki Mathabathe, in: *Handbooks in Advanced Manufacturing, Advanced Welding and Deforming*, Elsevier, Amsterdam, Netherlands, 2021, p.291-319.

[13] M. A. Javed, A. S. M. Ang, C. M. Bhadra, R. Piola, W. C. Neil, C. C. Berndt, M. Leigh, H. Howse, S. A. Wade, *Surface Coating Technology* **418** (2021). https://doi.org/10.1016/j.surfcoat.2021.127239

[14] S. Sivarajan, R. Padmanabhan, *Advances in Materials and Processing Technologies* **7** (2021) 227-240. https://doi.org/10.1080/2374068X.2020.1758605

[15] A. Scrivani , S. Ianelli , A. Rossi R. Groppetti , F. Casadei , G. Rizzi, *Wear* **250** (2001) 107-113. https://doi.org/10.1016/S0043-1648(01)00621-4

[16] D. Brabazon,S. Naher, P. Biggs, *Solid State Phenonena* **141-143** (2008) 255-260. https://doi.org/10.4028/www.scientific.net/SSP.141-143.255

[17] H. J. Shin, Y. T. Yoo, *Journal of Material Processing Technology* **201** (2008)342-347. https://doi.org/10.1016/j.jmatprotec.2007.11.232
[18] A. Gisario, M. Barletta, F. Veniali, *Optics Laser Technology* **44** (2012) 1942-1958. https://doi.org/10.1016/j.optlastec.2012.02.011
[19] J. C. Abboud, K. Y. Benyounis, A. G. Olabi, M. S. J. Hashmi, *Journal of Material Processing Technology* **182** (2007) 427-431. https://doi.org/10.1016/j.jmatprotec.2006.08.026
[20] M. A. Montealegra, G. Castro, P. Rey, J. Larias, P. Vasquez, M. Gonzalez, *Contemporary Materials* **I-1** (2010) 19-30. https://doi.org/10.5767/anurs.cmat.100101.en.019M
[21] P. Poza, C. J. Múnez, M. A. Garrido-Maneiro, S. Vezzù, S. Rech, A. Trentin, *Surface and Coatings Technology* **243** (2014) 51-57. https://doi.org/10.1016/j.surfcoat.2012.03.018
[22] V. C. Kumar, *Surface and Coatings Technology* **201** (2006) 3174-3180. https://doi.org/10.1016/j.surfcoat.2006.06.035
[23] Z. Y. Taha-al, M. S. J. Hashmi, B. S. Yilbas, *Journal of Material Processing Technology* **209** (2009) 3172-3181. https://doi.org/10.1016/j.jmatprotec.2008.07.027
[24] S.-H. Zhang,T.-Y. Cho, J.-H. Yoon, W. Fang, K.-O Song, M.-X. Li, Y.-K. Joo, C. G. Lee, *Materials Characterization* **59** (2008) 1412-1418. https://doi.org/10.1016/j.matchar.2008.01.003
[25] J. Suutala, J. Tuominen, P. Vuoristo, *Surface and Coatings Technology* **201** (2006) 1981-1987. https://doi.org/10.1016/j.surfcoat.2006.04.042
[26] Z. Liu, *Surface and Coatings Technology* **201** (2007) 7149-7158. https://doi.org/10.1016/j.surfcoat.2007.01.032
[27] A. Meghwal, C. C. Berndt, V. Luzin, C. Schulz, T. Crowe, H. Gabel, A. S. M. Ang, *Surface and Coatings Technology* **421** (2021) 127359. https://doi.org/10.1016/j.surfcoat.2021.127359
[28] A. A. Siddiqui, A. K. Dubey, *Optics Laser Technology* **134** (2021) 106619. https://doi.org/10.1016/j.optlastec.2020.106619
[29] A. G. M. Pukasiewicz, H. E. de Boer, G. B. Sucharski, R. F. Vaz, L. A. J. Procopiak, *Surface and Coatings Technology* **327** (2017) 158-166. https://doi.org/10.1016/j.surfcoat.2017.07.073
[30] A. K. Gujba, M. S. Mahdipoor, M. Medraj, *Wear* **484-485** (2021) 203904. https://doi.org/10.1016/j.wear.2021.203904
[31] M. Michalak, L. Latka, P. Sokolowski, F.-L. Toma, H. Myalska, A. Denoirjean, H, Ageorges, *Surface and Coatings Technology* **404** (2020) 126463. https://doi.org/10.1016/j.surfcoat.2020.126463
[32] G. Prashar, H. Vasudev, *Materials Today: Proceedings* **26(2)** (2020) 1131-1135. https://doi.org/10.1016/j.matpr.2020.02.226
[33] H. Vasudev, G. P. L. Thakur, A. Bansal, *Surface Review and Letters* **29(2)** (2022) 2250017. https://doi.org/10.1142/S0218625X22500172
[34] D. D. Kumar, P. Grewal, J. Singh, *Corrosion Reviews* **39** (2021) 243-268. https://doi.org/10.1515/corrrev-2020-0043
[35] G. Prashar, H. Vasudev, *Surface and Coatings Technology* **439** (2022) 128450 https://doi.org/10.1016/j.surfcoat.2022.128450
[36] T. S. Sidhu, S. Prakash, R. D. Agrawal, *Materials Science* **41(6)** (2005) 805-823. https://doi.org/10.1007/s11003-006-0047-z
[37] B. S. Yilbas, S. S. Akhtar, *Journal of Material Processing Technology* **212** (2012) 2569-2577. https://doi.org/10.1016/j.jmatprotec.2012.07.012
[38] B. S. Yilbas, A. F. M. Arif, M. A.Gondal, *Journal of Material Processing Technology* **164-165** (2005) 964-957. https://doi.org/10.1016/j.jmatprotec.2005.02.091
[39] *Image J* https://imagej.net/software/imagej/ (5/31/2022)